**iScience, Volume *24***

## Supplemental Information

# E-cigarettes compromise the gut barrier and trigger inflammation

**Aditi Sharma, Jasper Lee, Ayden G. Fonseca, Alex Moshensky, Taha Kothari, Ibrahim M. Sayed, Stella-Rita Ibeawuchi, Rama F. Pranadinata, Jason Ear, Debashis Sahoo, Laura E. Crotty-Alexander, Pradipta Ghosh, and Soumita Das**

## Supplementary Online Information

# MATERIALS AND METHODS

## Key Resource Table

| REAGENT or RESOURCE | SOURCE | IDENTIFIER |
|---|---|---|
| **Biological Samples** | | |
| C57B/L6 mice | ENVIGO/HARLAN | |
| Adherent Invasive Escherichia coli strain LF82 (*AIEC*-LF82) | Arlette Darfeuille-Michaud, Inserm | (Chassaing and Darfeuille-Michaud, 2011) (Darfeuille-Michaud et al., 2004) Darfeuille-Michaud, A |
| Human tissue biopsies | HUMANOID CoRE<br>VA hospital, San Diego | UCSD HRPP Project ID190105 |
| | | |
| **Primers (Mouse/Human)** | Forward primer (3'- 5') | Reverse primer (3'- 5') |
| Mouse 18S qPCR primers | GTAACCCGTTGAACCCCATT | CCATCCAATCGGTAGTAGCG |
| Mouse ZO-1 qPCR primers | GGGAGGGTCAAATGAAGACA | GGCATTCCTGCTGGTTACAT |
| Mouse IL-6 qPCR primers | CCCCAATTTCCAATGCTCTCC | CGCACTAGGTTTGCCGAGTA |
| Mouse IL-1b qPCR primers | GAAATGCCACCTTTTGACAGT | CTGGATGCTCTCATCAGGACA |
| Mouse TNF-alpha qPCR primers | CCACCACGCTCTTCTGTCTA | AGGGTCTGGGCCATAGAACT |
| Mouse IL-8 qPCR primers | CCTGCTCTGTCACCGATG | CAGGGCAAAGAACAGGTCAG |
| Mouse MCP-1 qPCR primers | AAGTGCAGAGAGCCAGACG | TCAGTGAGAGTTGGCTGGTG |
| Mouse Occludin qPCR primers | CCTCCAATGGCAAAGTGAAT | CTCCCCACCTGTCGTGTAGT |
| Mouse Claudin-1 qPCR primers | CCCCCATCAATGCCAGGTATG | AGAGGTTGTTTTCCGGGGAC |
| Mouse Claudin-2 qPCR primers | CCTTCGGGACTTCTACTCGC | TCACACATACCCAGTCAGGC |
| Human IL-8 qPCR primers | GAGCACTCCATATGGCACAAA | ATGGTTCCTTCCGGTGGT |
| Human IL-6 qPCR primers | CCAGAGCTGTGCAGATGAGT | CTGCAGCCACTGGTTCTGT |
| Human IL-1b qPCR primers | CCACAGACCTTCCAGGAGAATG | GTGCAGTTCAGTGATCGTACAGG |
| Human MCP-1 qPCR primers | AGTCTCTGCCGCCCTTCT | GTGACTGGGGCATTGATTG |
| Human ZO-1 qPCR primers | CGGTCCTCTGAGCCTGTAAG | GGATCTACATGCGACGACAA |
| Human Occludin qPCR primers | TCAGGGAATATCCACCTATCACTTCAG | CATCAGCAGCAGCCATGTACTCT TCAC |
| | | |
| **Software programs** | | |
| Prism | Graphpad | https://www.graphpad.com/scientific-software/prism/ |
| Illustrator | Adobe | https://www.adobe.com/products/illustrator.html |
| Leica Application Suite X (LAS X) | Leica Microsystems | https://www.leica-microsystems.com/products/microscope-software/p/leica-las-x-ls/ |
| Image J | FIJI | https://imagej.net/Welcome |
| AxioImager Z1 microscope | Carl Zeiss MicroImaging | |
| | | |
| **Chemicals and Reagents** | | |
| Direct-zol RNA Miniprep Kit | Zymo Research | R2052 |
| Human IL-8/CXCL8 DuoSet ELISA | R&D systems | DY208 |
| Human CCL2/MCP-1 DuoSet ELISA | R&D systems | DY279 |
| Zinc Formalin Fixative | Fischer Scientific | 23313096 |
| DMEM with 10% FBS | Thermo Fisher Scientific | 11995073 |
| Fetal bovine serum | SIGMA-Aldrich | F2442-500ML |
| SB431542 (an inhibitor for TGF-β type I receptor | Bio-Techne Sales corp | 1614/50 |
| Y27632 (ROCK inhibitor) | Tocris | 1254 |
| Advanced DMEM/F12 | Thermo Fisher Scientific | 12634028 |

| | | |
|---|---|---|
| Trypsin | Thermo Fisher Scientific | 15090046 |
| Prolong Gold | Thermo Fisher Scientific | P36930 |
| DNA/RNA Oxidative Damage ELISA Kit | Cayman Chemical, USA | 501130 |
| Collagenase type II | Invitrogen | 17101015 |
| 70-µm cell strainer | Thermo Fisher Scientific | 22-363-548 |
| Matrigel | CORNING | 354234 |
| Gentamicin | Thermo Fisher Scientific | 15750060 |
| Transwell inserts | Thermo Fisher Scientific | 07-200-154 |
| qScript™ cDNA SuperMix | Quantabio | 101414-108 |
| Methanol | ACS | EM-MX0485-3 |
| Triton X-100 | SIGMA-Aldrich | X100-500ML |
| Trypan Blue | Thermo Fisher Scientific | 15250061 |
| HTS Transwell®-96 Permeable Support with 0.4 µm PET Membrane | Corning | 7369 |
| | | |
| **Antibodies** | | |
| Anti-Occludin mouse monoclonal antibody (1:500) | Invitrogen | 331500 |
| Anti-ZO-1 rabbit polyclonal antibody (1:500) | GeneTex | GTX108627 |
| Alexa Fluor 594 conjugated goat anti-rabbit IgG (1:500) | Invitrogen | A11012 |
| Alexa Fluor 488 conjugated goat anti-mouse IgG (1:500) | Invitrogen | A11001 |
| DAPI (1:1000) | Invitrogen | D1306 |
| | | |
| **Instruments** | | |
| Countess II Automated Cell Counter | Thermo Fisher Scientific | AMQAX1000 |
| Epithelial Volt/Ohm (TEER) Meter | WPI | SKU EVOM2 |
| Automated TEER Measurement System (REMS AutoSampler, Version 6.02) | WPI | SYS-REMS |
| Corning HTS Transwell-96 Electrode | WPI | REMS-96C |
| Leica Automated Inverted Microscope | Leica Microsystems | Leica DMI4000 B |

All methods involving human and animal subjects were performed in accordance with the relevant guidelines and regulations of the University of California San Diego and the NIH research guidelines.

**Murine E-Cigarette aerosol exposures:** Six to eight-week-old male or female C57BL/6 (Envigo) were acclimatized to the SciReq whole body exposure inhalation system for 30 min a day for 3 days prior to beginning e-cigarette exposures. Mice were placed into individual slots in the whole-body exposure system and exposed for 4 sec every 20 sec for 1 h/day, 5 d/wk, for 1 wk or 12 wks. Mice received e-cigarette vapor produced from e-liquid containing 70/30 propylene glycol and glycerol with nicotine (Sigma) at a concentration of 6 mg/mL or without nicotine. At the end of the exposure period, mice were anesthetized with 10mg/kg and 100 mg/kg of xylazine and ketamine, respectively.

**Preparation of E-cigarette vapor-infused media:** E-liquid mixture of 70% propylene glycol and 30% glycerol and 6mg/mL nicotine (purchased from Sigma) without flavors or additives were used. E-cigarette atomizer and the rechargeable battery were obtained from Scireq. The atomizer contains a Kangertech Subtank Plus (7mL), with a 0.15 ohm coil. Fresh e-cig vapor-infused media was created by activating the battery via application of negative pressure by the InExpose system (SciReq), the e-liquid was heated and drawn through the internal atomizer and then into a 60 ml syringe containing 10 ml of wash media (DMEM/F12 with HEPES, 10% FBS). The wash media was exposed to 50mLs of e-cig vapor generated from the vaporization of the e-cig liquid, (with or without 6 mg/ml nicotine) followed by a 12-second shake; this is repeated 30 times.

**Human subjects:** Human ileum and colonic biopsies were collected from healthy subjects undergoing routine colonoscopy for colon cancer screening using the protocol approved by the Human Research Protection Program Institutional Review Board (Project ID# 190105). For all the deidentified human subjects, information including age, ethnicity, gender, previous history of the disease, and the medication was collected from the chart following the rules of HIPAA. Each human participant was recruited to the study following an approved human research protocol and signed a consent form approved by the Human Research Protection Program at the University of California, San Diego. Each donor agrees that their gastro-intestinal specimens will be used to generate an enteroid line at UC San Diego's HUMANOID$^{TM}$ Center of Research Excellence (CoRE) for functional studies.

**Isolation of enteroids from mouse and ileum and colonic specimens of healthy human:** Intestinal crypts, comprised of crypt-base columnar (CBC) cells, were isolated from both colonic tissue of mice; and human colonic and ileal tissue specimens using the previously published paper (Ghosh et al., 2020; Sayed et al., 2020c). In brief, intestinal crypts were dissociated from tissues by digesting with collagenase type I (2 mg/mL solution containing gentamicin 50 ug/mL). The plate was incubated in a $CO_2$ incubator at 37°C, mixing every 10 minutes with vigorous pipetting in-between incubations, while monitoring the release of single epithelial units from tissue structures by light microscopy. To inactivate collagenase, wash media (DMEM/F12 with HEPES, 10% FBS) was added to cells, filtered through a 70 µM cell strainer, centrifuged at 200g for 5 min and then the supernatant was aspirated, leaving a cell pellet. The number of viable intestinal stem cells was determined by the Trypan Blue Exclusion method using Countess II Automated Cell Counter. Epithelial units were resuspended in matrigel and 15µl of cell-Matrigel suspension was added to the wells of a 24-well plate on ice and incubated upside-down in a 37°C $CO_2$ incubator for 10 min, which allowed for polymerization of the matrigel. After 10 min of incubation, 500µL of 50% Conditioned Media (CM, prepared from L-WRN cells with Wnt3a, R-spondin and Noggin, ATCC® CRL-3276™ (Miyoshi and Stappenbeck, 2013) containing 10 µM Y27632 and 10 µM SB431542 were added to the suspension. For the human colonic specimens, an in-house

proprietary cocktail was added to the above media. The medium was changed every 2 days and the enteroids were either expanded or frozen in liquid nitrogen for biobanking.

**Preparation of Enteroid-derived monolayers (EDMs):** EDMs were prepared by dissociating single cells from enteroids and plated either in 24-well or 96-well transwell with a 0.4 μm pore polyester membrane coated with diluted Matrigel (1:40) in 5% conditioned media as done before (Ghosh et al., 2020; Sayed et al., 2020c). The single-cell suspension was seeded at a density of approximately $2x10^5$ cells/well (in case of 24-well) or $8x10^4$ cells/well (in case of 96-well) and EDMs were differentiated for 2-3 days in 5% CM. The media was changed every 24 hours and monitored under a light microscope to evaluate the EDM generation and quality. As expected, the expression of EDMs showed a significant reduction of the stemness marker lgr5 in EDMs (Ghosh et al., 2020; Sato et al., 2009; Sayed et al., 2020c).

**The treatment of enteroid-derived monolayers (EDMs) with e-cigarette vapor-infused media for functional assays:** The polarized differentiated EDMs were treated with media that was infused with either nicotine-free e-cigarette or with 6 mg/mL nicotine-containing e-cigarettes by adding the vapor-infused media to the basolateral compartment of the transwells for the indicated times. The cells were either stained for confocal microscopy or used for measurement of transepithelial electrical resistance (TEER) or mRNA isolation; and for the collection of supernatants from apical and basolateral sides.

**The measurement of Transepithelial electrical resistance (TEER):** Two different methods were used for the measurement of TEER in low- (LTP) and high-throughput (HTP) modes.

*Manual, LTP*: In 24-well, TEER was measured at 0 h, 1 h, 4 h, 8 h, and 24 h, following exposure to e-cigarette vapor infused media using the STX2 electrodes with digital readout by EVOM2 (WPI).

*Automated, HTP*: The TEER of 96-well transwell plate with EDMs was measured using WPI automated TEER Measurement System. WPI REMS-96C recording electrode was used to record TEER, compatible with Corning 96-well plate format. REMS-96C recording electrode was sterilized in 70% Ethanol, followed by rinse in PBS and media. The REMS-96C apical electrode was calibrated to measure TEER approximately 1 mm above transwell membrane. Transwell-read time set to 12sec/well. Once set-up complete, plate removed from incubator and TEER measured directly afterward; the same read sequence was repeated every subsequent read to mitigate TEER artifacts due to temperature fluctuations. TEER recorded by REMS AutoSampler were saved as .txt files; raw TEER values (in Ωs), are converted to normalized TEER values by Raw TEER in ohms (Ω) x surface area of transwell in $cm^2$ = ohms. $cm^2$ (SA=0.143 $cm^2$ for 96-well and 0.33 $cm^2$ for 24-well).

**Infection of EDMs with Adherent Invasive *E. coli (AIEC*-LF82*):*** Adherent Invasive *Escherichia coli* strain LF82 (*AIEC*-LF82), isolated from the specimens of Crohn's disease patient, was obtained from Arlette Darfeuille-Michaud (Darfeuille-Michaud et al., 2004). For experimental use, a single colony was inoculated into LB broth and grown for 8 h under aerobic conditions and then under oxygen-limiting conditions overnight. 24h following treatment with e-cig vaped media, cells in the transwells were infected apically with a multiplicity of infection (moi) of 30 for 3 h. For gentamicin protection assay, bacteria were removed after 3h and treated with 200 μg/ml of gentamicin for 90 minutes, followed by serial dilution in 1x PBS and plating on LB agar plates. Colonies were counted the next day to measure colony forming unit per ml (cfu/ml)

**RNA isolation and qRT-PCR:** RNA was isolated from mouse colon tissues and EDMs followed by cDNA synthesis, as per manufacturer's instructions. Quantitative Real-Time PCR was conducted for target genes and normalized to housekeeping gene 18S rRNA. Fold change of treatment conditions was determined relative to the control condition. All primer sequences used in the study are provided in the key resource Table above.

**RNA Seq and pathway enrichment analyses:** RNASeq data was processed via kallisto (Bray et al., 2016) using the human genome build GRCh38 ensembl version 94 and corresponding genome annotation file to compute TPM (Transcripts Per Millions) (Li and Dewey, 2011; Pachter, 2011) values. We used log2(TPM+1) to compute the final log-reduced expression values. StepMiner (Sahoo et al., 2007) algorithm was used to compute a threshold for the high and low values for each gene. To generate the heatmap, a modified Z-score approach with StepMiner threshold (formula = (expr -SThr)/3*stddev) was used to further normalize the gene expression values. R version 3.2.3 (2015-12-10) was used to perform all statistical tests. We used python scipy.stats.ttest_ind package (version 0.19.0) with Welch's Two Sample t-test (unpaired, unequal variance (equal_var=False), and unequal sample size) parameters. For multiple hypothesis correction, *p* values were adjusted with statsmodels.stats.multitest.multipletests (fdr_bh: Benjamini/Hochberg principles). R statistical software (R version 3.6.1; 2019-07-05) was used to independently validate the results.

Over-representation (KEGG, GO, etc) analyses were carried out using the **g:GOSt** platform on p:Profiler (https://biit.cs.ut.ee/gprofiler/gost). The g:GOSt platform performs functional over-representation analysis (ORA) on input gene lists and identify statistically significantly enriched terms. The website curates data from Ensembl database and include pathways from KEGG, Reactome and WikiPathways; tissue specificity from Human Protein Atlas; protein complexes from CORUM and human disease phenotypes from Human Phenotype Ontology.

The RNA Seq dataset associated with this study can be accessed at NCBI GEO (GSE161521).

**H& E staining:** Colonic specimens were rinsed with phosphate-buffered saline (PBS) and fixed in zinc formalin for 24 h and embedded in paraffin. Paraffin sections (4 μm) were cut and de-waxed prior to immune-histochemical staining. Sections were stained with hematoxylin/eosin (H&E). Standard light microscopy was used to image tissue sections.

**ELISA:** Supernatant was collected from basolateral sides of EDMs and was examined for secreted cytokines, including IL-8 and MCP-1. These studies were done exactly as described previously (Sayed et al., 2020b; Sayed et al., 2020c) using biolegend kit as per manufacturer's protocol.

**Measurement of oxidative DNA/RNA damage:** The amount of oxidative DNA damage in untreated and e-cigarette treated EDMs before and after infection were quantified according to the manufacturer's instruction and previously published papers from others (Gao et al., 2019; Rodrigues et al., 2017) and from our own group (Sayed et al., 2020a; Sayed et al., 2020b). Briefly, supernatant from treated EDMs was used to detects oxidized guanine species: 8-hydroxy-2′-deoxaguanosine from DNA, and 8-hydroxyguanine from either DNA or RNA.

**Immunofluorescence staining:** Following the final TEER measurement, the media was removed from apical and basolateral compartments of all EDMs and gently washed 3 times with room temperature PBS, fixed with cold 100% methanol at 20°C for 20 min. Afterward, methanol was removed and washed with blocking buffer (0.1% Triton TX-100, 2 mg/mL BSA diluted in PBS) to permeabilize EDMs and to incubate with the following primary antibodies: ZO-1 (1:500) and Occludin (1:500). Primary antibodies were removed and washed with PBS 3 times for 5 min each time; after which the following secondary antibodies were added: Alexa Fluor 594 conjugated goat anti-rabbit IgG, Alexa Fluor 488 conjugated goat anti-mouse IgG and DAPI. Secondary antibodies were removed and washed with PBS 3 times for 5 min each time. To preserve fluorescence, monolayers were treaeded with Prolong Gold antifade reagent and stored at 4°C until imaged. Confocal Microscope with a 40x objective lens was used to image the stained EDMs. Z-stack images were acquired by successive 1 μm depth Z-slices of EDMs in the desired confocal channels of Leica TCS SP5 Confocal Microscope as done previously (Ghosh et al., 2020). Fields of view that were representative of a given transwell were determined by randomly imaging 3 different fields. Z-slices of a Z-stack were overlaid to create maximum intensity projection images; all images were processed using FIJI (Image J) software.

**Statistical analysis**

TEER, qPCR and ELISA results were expressed as the mean ± SEM and compared using a one-way ANOVA with Tukey's test or Mann-Whitney test. GraphPad Prism was used to analyze results and p-values $< 0.05$ was considered significant.

## SUPPLEMENTARY TABLES

### List of downregulated genes (n = 75)

| | | | | | | | | | |
|---|---|---|---|---|---|---|---|---|---|
| B830042I05RIK | OTUD4 | D430018E03RIK | GM20476 | PKN2 | AFTPH | SCYL3 | EHF | 1700028B04RIK | GM25219 |
| MADCAM1 | GM43213 | GM17733 | 4732463B04RIK | ASXL2 | IGHV 1-26 | TRIM30A | HADHA | AW822252 | SMG1 |
| GM31774 | ZBED6 | CDK13 | PTAR1 | TRIM36 | PRPF40A | SLC33A1 | ACNAT1 | ZFP871 | TRPV3 |
| GM12511 | RPS10-PS1 | HAO2 | 1700120E14RIK | RDH16F2 | NAIP3 | RANBP2 | ZAN | ABCG2 | TNPO1 |
| GM26812 | VAMP7 | GM11945 | MAP3K2 | TECPR1 | LY6C2 | TMEM181B-PS | ETFDH | GM26711 | SLC12A5 |
| ZFP748 | SLC12A3 | GM44216 | AL611930.1 | ALG13 | NUFIP2 | GP2 | SIRT3 | PREPL | GM15693 |
| CLDN12 | RBM45 | SH3GL2 | MZB1 | USP53 | RCOR1 | UNC13B | ATP6V0A2 | TRIML1 | GM9938 |
| MOB1B | MYB | A1CF | EYA3 | GAL3ST2c | | | | | |

### List of upregulated genes (n = 120)

| | | | | | | | | | |
|---|---|---|---|---|---|---|---|---|---|
| CNIH2 | SBSN | WFDC12 | GM15519 | TMPRSS11A | STFA1 | CTCFLOS | TNNC2 | ADIG | CYP1A1 |
| LCE1D | SERPINB12 | GM26751 | PIN1 | FAM178B | ENDOU | IL31RA | 1700003F12RIK | CCDC27 | DAPL1 |
| MCPT4 | GM32772 | CNFN | KRT13 | KRT10 | DEFB14 | CSTA1 | MARC1 | GM15551 | GM94 |
| GM12496 | RETN | GP1bb | KRT6B | LGALS7 | EAR2 | BORCS5 | Hp | GM10108 | LCE1A2 |
| LEP | CRCT1 | GM48007 | 9330161L09RIK | AC164431.1 | HOXD3OS1 | LCE3F | GM11772 | CALM4 | PRKAB2 |
| LCE3E | CCL8 | APOC1 | SLS36A2 | LCE3B | LCE3A | DKKL1 | KLK8 | SPRR1A | LCE3C |
| IL1R2 | TAGLN | SULT5A1 | 2300002M23RIK | LIPE | ARXES1 | SLURP1 | DEFB6 | DEFB4 | NNAT |
| SMOC1 | EYA1 | SCD1 | RTL5 | LOR | MT4 | DISC1 | NNMT | ARG1 | GM47507 |
| KRTAP20-2 | ATP2A1 | GAL3ST4 | TMEM45A | TRIM29 | TLCD2 | FLG | SERPINB1C | S100A4 | EMB |
| CAR3 | SPRR4 | SPRR3 | LCE1A1 | FABP4 | FABP5 | RNASE2B | GLB1L2 | LCE1G | FCOR |
| STFA3 | KRT1 | A230028O05RIK | KRT5 | KRT4 | FAM25C | APOL6 | KRT9 | APOBR | RNF165 |
| GM49339 | ADIPOQ | PLIN1 | ASPRV1 | ILK | ADRB3 | GM45716 | SERPINB3a | GLRX5 | BC100530 |

**Supplementary Table S1 (related to Fig 2):** Differentially regulated gene clusters in mice colon vaped with e-cigarette alone, versus e cigarette with nicotine.

**SUPPLEMENTARY FIGURES AND LEGENDS**

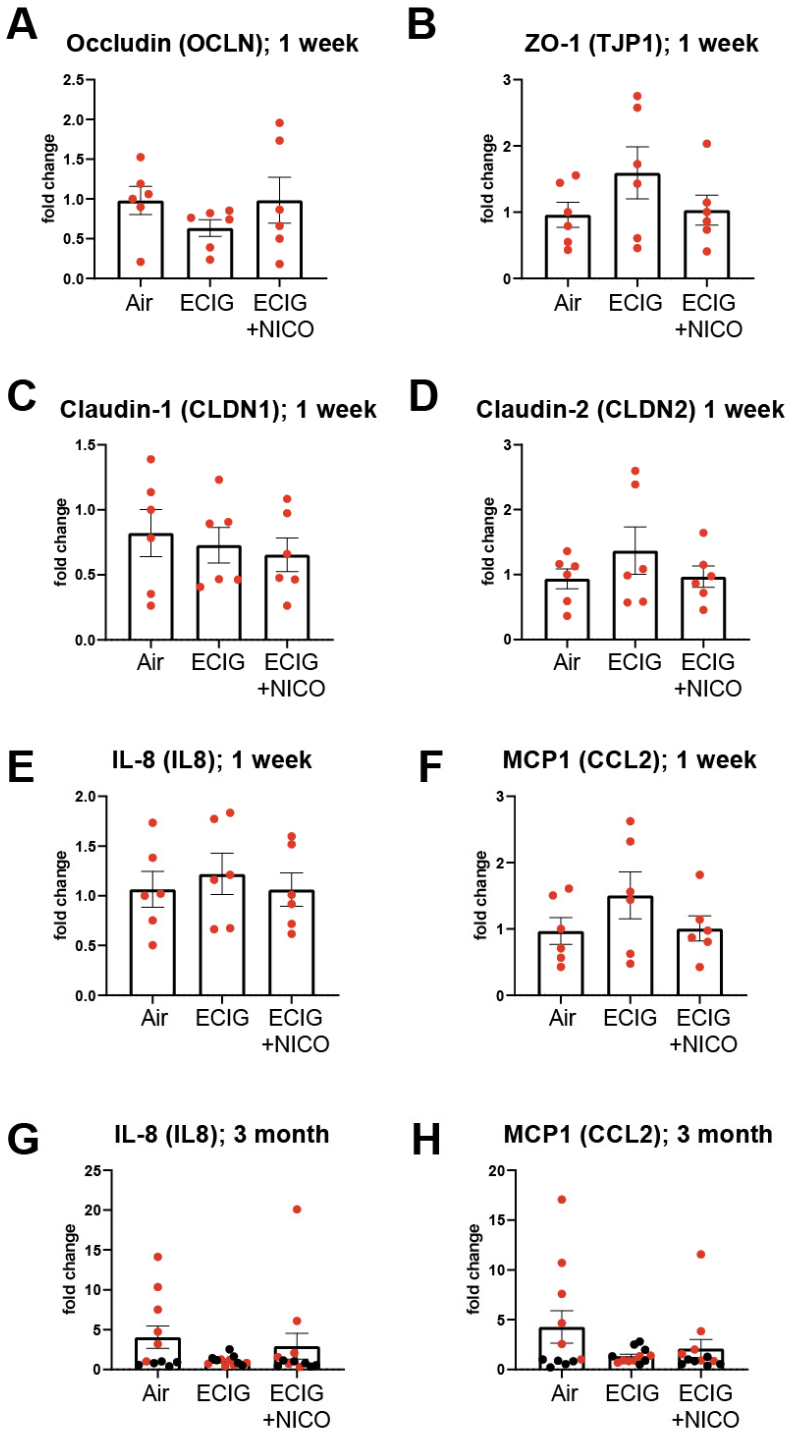


**Figure S1. Gene expression changes after acute (1 week) or chronic (3 mo) of vaping (related to Fig 1).** C57BL/6 mice were vaped using a special vaping chamber with MOD brand e-cigarette vapors (see **Fig 1A**), with (ECIG + NICO) and without (ECIG) 6 mg/ml nicotine for 1 week or 3 months by following specific regimen (details in methods), followed by isolation of the distal colon. The graphs represent the relative fold change in mRNA expression of tight junction markers (**A-D**) and pro-inflammatory cytokines (**E-H**) from 2-3 independent experiments with at least 4-5 mice/group of each experiment (Male mice = black data points; Female mice = red data points). Air = air control. Data represent as mean ± SEM. One-way ANOVA with Tukey's test was performed *$p < 0.05$, **$p < 0.01$ and ***$p < 0.001$.

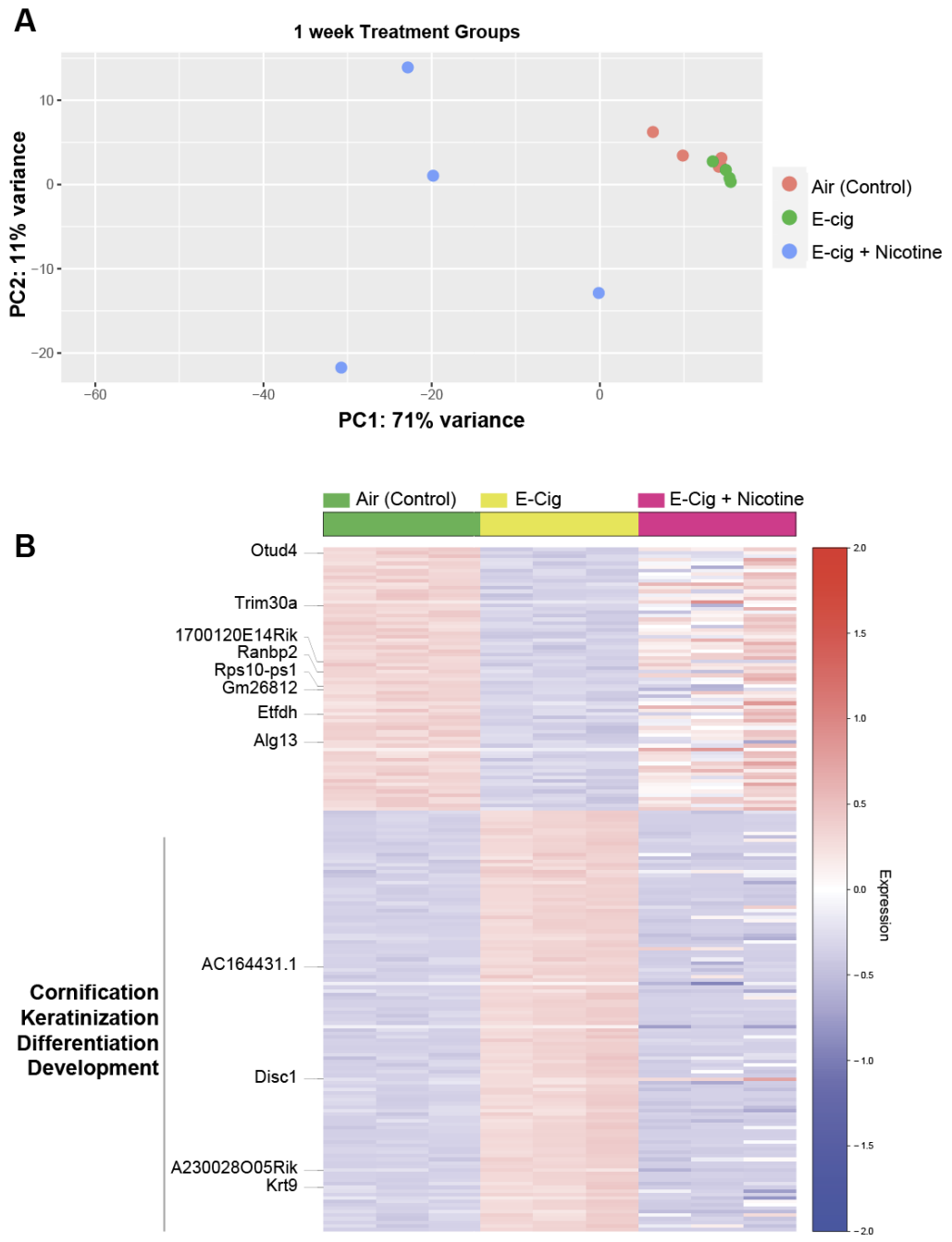


**Figure S2**. **Genes differentially expressed in mouse colon exposed to air or electronic cigarette (ECIG) vapors with and without nicotine (related to Fig 2)**. **A.** Principal component analysis of all 195 (75+120) genes by median absolute deviation. Colon exposed to e-cig vapors (green; n=4), e-cig with nicotine (purple, n =4), or Air (red; n=4). E-cig with nicotine samples differ from air controls and e-cig alone samples along with the first principal component, accounting for 71% of the variability in gene expression. **B.** Heatmap selectively highlighting those genes that are differentially expressed in air control (green) vs. e-cig alone (yellow) groups that are not rescued in the nicotine-containing e-cig group (magenta), as opposed to the large majority of them are indeed returned to levels in the control group (see **Fig 2B**). The upregulated genes support pathways (KEGG analysis) that concern differentiation, cornification and keratinization in the colon.

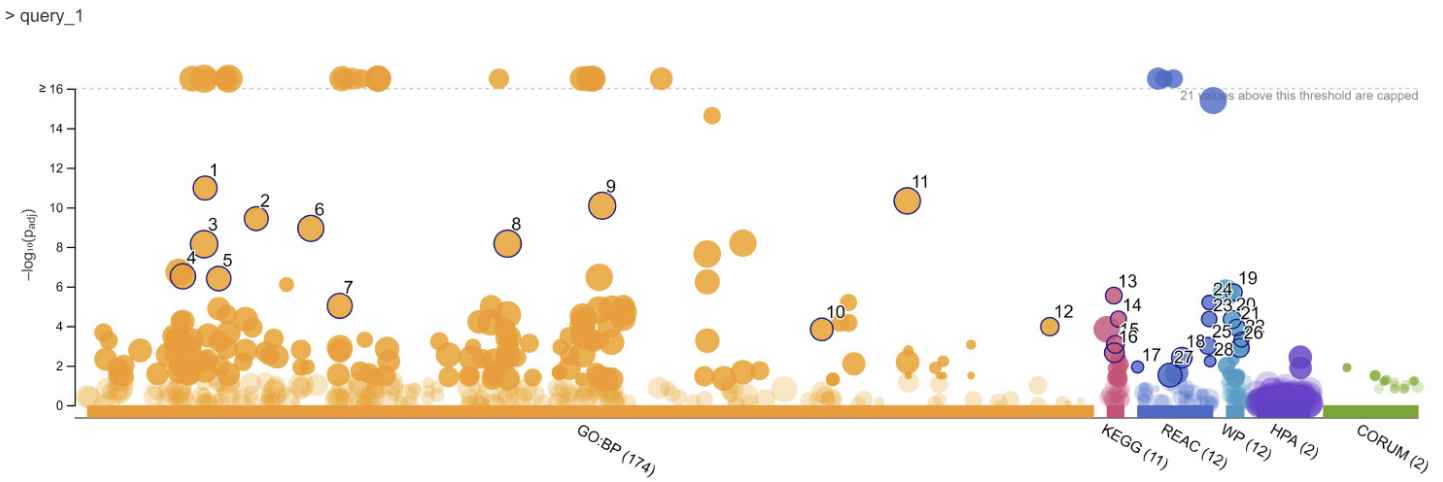


| ID | Source | Term ID | Term Name | $p_{adj}$ (query_1) |
|---|---|---|---|---|
| 1 | GO:BP | GO:0008219 | cell death | $1.060\times10^{-11}$ |
| 2 | GO:BP | GO:0012501 | programmed cell death | $3.723\times10^{-10}$ |
| 3 | GO:BP | GO:0008152 | metabolic process | $7.294\times10^{-9}$ |
| 4 | GO:BP | GO:0006950 | response to stress | $3.077\times10^{-7}$ |
| 5 | GO:BP | GO:0009605 | response to external stimulus | $3.978\times10^{-7}$ |
| 6 | GO:BP | GO:0019538 | protein metabolic process | $1.161\times10^{-9}$ |
| 7 | GO:BP | GO:0023051 | regulation of signaling | $9.560\times10^{-6}$ |
| 8 | GO:BP | GO:0044238 | primary metabolic process | $6.869\times10^{-9}$ |
| 9 | GO:BP | GO:0050896 | response to stimulus | $8.315\times10^{-11}$ |
| 10 | GO:BP | GO:0098542 | defense response to other organism | $1.476\times10^{-4}$ |
| 11 | GO:BP | GO:1901564 | organonitrogen compound metabolic process | $4.735\times10^{-11}$ |
| 12 | GO:BP | GO:1990845 | adaptive thermogenesis | $1.076\times10^{-4}$ |
| 13 | KEGG | KEGG:03320 | PPAR signaling pathway | $2.891\times10^{-6}$ |
| 14 | KEGG | KEGG:04923 | Regulation of lipolysis in adipocytes | $4.425\times10^{-5}$ |
| 15 | KEGG | KEGG:04152 | AMPK signaling pathway | $8.463\times10^{-4}$ |
| 16 | KEGG | KEGG:04060 | Cytokine-cytokine receptor interaction | $2.201\times10^{-3}$ |
| 17 | REAC | REAC:R-HSA-16... | AMPK inhibits chREBP transcriptional activation ac... | $1.171\times10^{-2}$ |
| 18 | REAC | REAC:R-HSA-67... | Neutrophil degranulation | $3.959\times10^{-3}$ |
| 19 | WP | WP:WP3942 | PPAR signaling pathway | $1.976\times10^{-6}$ |
| 20 | WP | WP:WP236 | Adipogenesis | $4.642\times10^{-5}$ |
| 21 | WP | WP:WP1403 | AMP-activated Protein Kinase (AMPK) Signaling | $1.179\times10^{-4}$ |
| 22 | WP | WP:WP3965 | Lipid Metabolism Pathway | $4.876\times10^{-4}$ |
| 23 | REAC | REAC:R-HSA-89... | Triglyceride metabolism | $4.414\times10^{-5}$ |
| 24 | REAC | REAC:R-HSA-16... | Triglyceride catabolism | $6.438\times10^{-6}$ |
| 25 | REAC | REAC:R-HSA-38... | Transcriptional regulation of white adipocyte differ... | $1.004\times10^{-3}$ |
| 26 | WP | WP:WP2877 | Vitamin D Receptor Pathway | $1.275\times10^{-3}$ |
| 27 | REAC | REAC:R-HSA-16... | Immune System | $3.004\times10^{-2}$ |
| 28 | REAC | REAC:R-HSA-89... | VLDL clearance | $5.944\times10^{-3}$ |

**Figure S3**. **Gene ontology (GO) analysis of differentially expressed genes the colons of mice exposed to e-cig compared to air controls (related to Fig 2).** Manhattan-like plots (top) represent the statistical enrichment (bottom) of pathways were generated using the list of differentially expressed genes and g:GOSt, a core of the g:Profiler that uses statistical enrichment analysis to interpret the functional relevance of gene signatures. The x-axis represents functional terms that are grouped and color-coded by data sources (e.g. GO biological process, orange; KEGG, magenta; Reactome, blue, etc). The y-axis shows the adjusted enrichment p-values in a negative log10 scale. The light circles represent insignificant terms (if available).

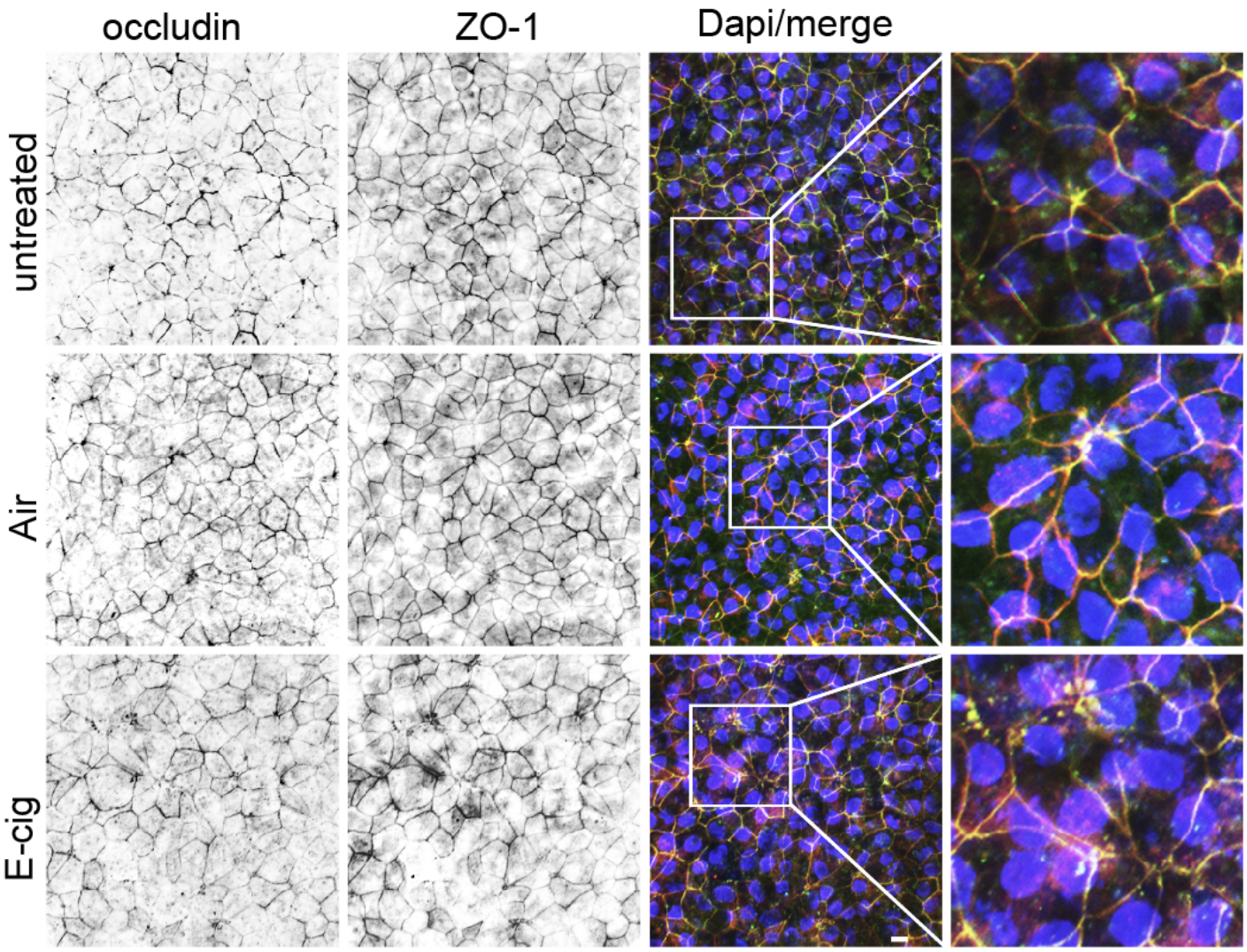


**Figure S4. Confocal microscopic analysis of human EDMs after chronic exposure to e-cig vapor-infused media (related to Fig 3).** Representative images show Occludin (a TJ marker; green), ZO-1(a TJ marker; red) and DAPI (blue, nuclei) in colonic EDMs either left untreated (top) for 24 h or exposed for the same duration to air (middle) or e-cig (bottom)-vapor-infused media. Scale bar = 10 μm. Cropped images on the right are presented in **Fig 3E**.

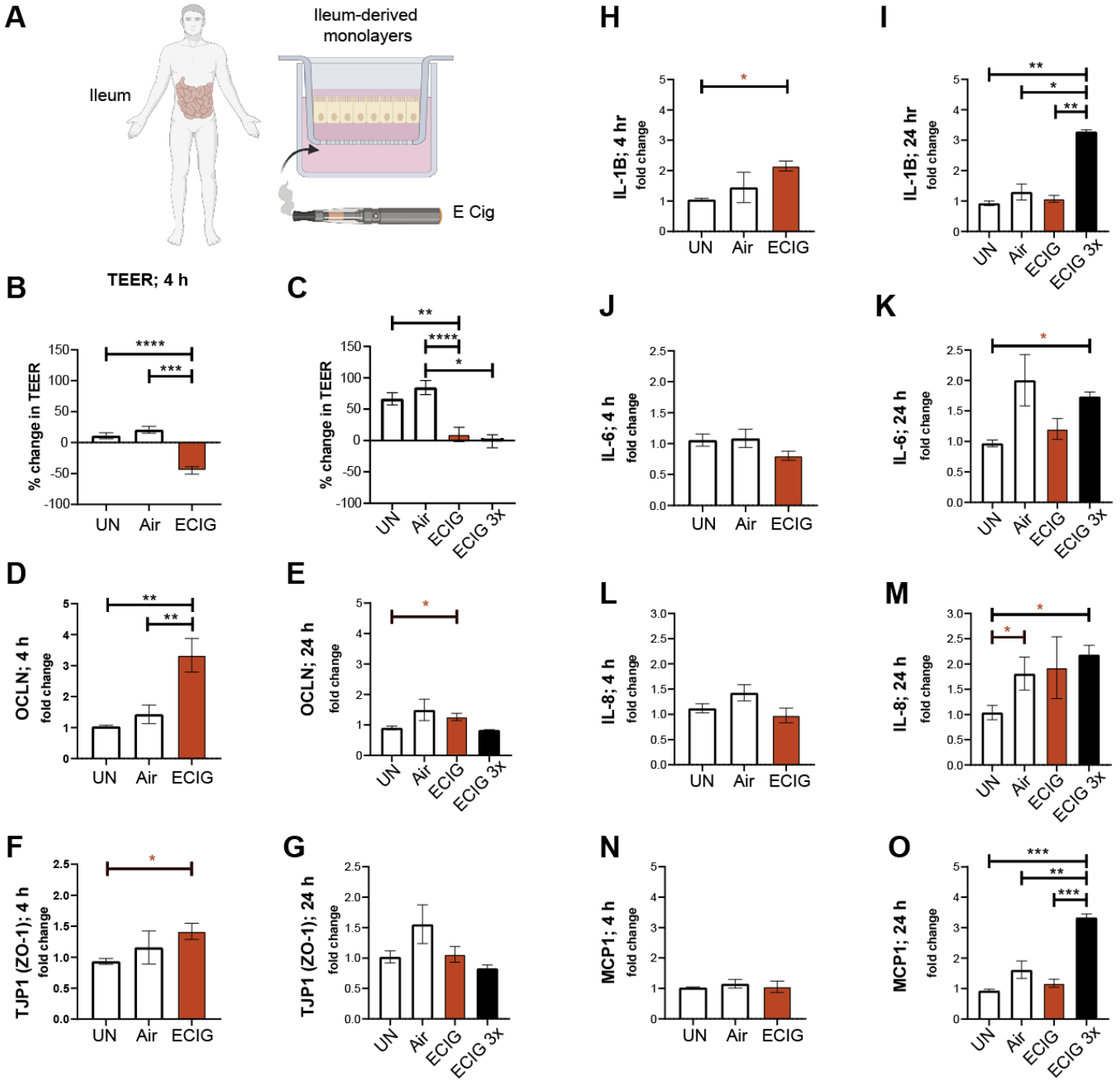


**Figure S5. Nicotine-free e-cig disrupts the human ileal epithelial barrier, triggers inflammation (related to Fig 4). A.** Schematic displays how enteroids isolated from ileal biopsies of healthy humans were differentiated into polarized enteroid-derived monolayers (EDMs) and exposed to e-cig vapor- infused media on the basolateral side. **B-C**. EDMs were either grown in normal media (UN) or treated with air-infused media (Air) or e-cig vapor-infused media (e-cig) and transepithelial electrical resistance (TEER) was measured over time. The graphs represented the percent change in $\Omega^*cm^2$ from three independent experiments and displayed as mean ± SEM. Healthy ileal EDMs were maintained in media or treated with air-infused media or e-cigarette vapor- infused media. After acute exposure of 4 h and chronic exposure of 24 h, mRNA expression was measured after single or multiple exposures. The graphs represented the relative fold change compared to the EDM grown in normal media (UN) and mRNA expression of tight junction markers (**D-G**) and inflammatory cytokines (**H-O)** was measured from at least three independent experiments and displayed as mean ± SEM. One-way ANOVA with Tukey's test (black *) and Mann-Whitney (red *) test was performed *$p < 0.05$, **$p < 0.01$ ,***$p < 0.001$ and ****$p < 0.0001$.

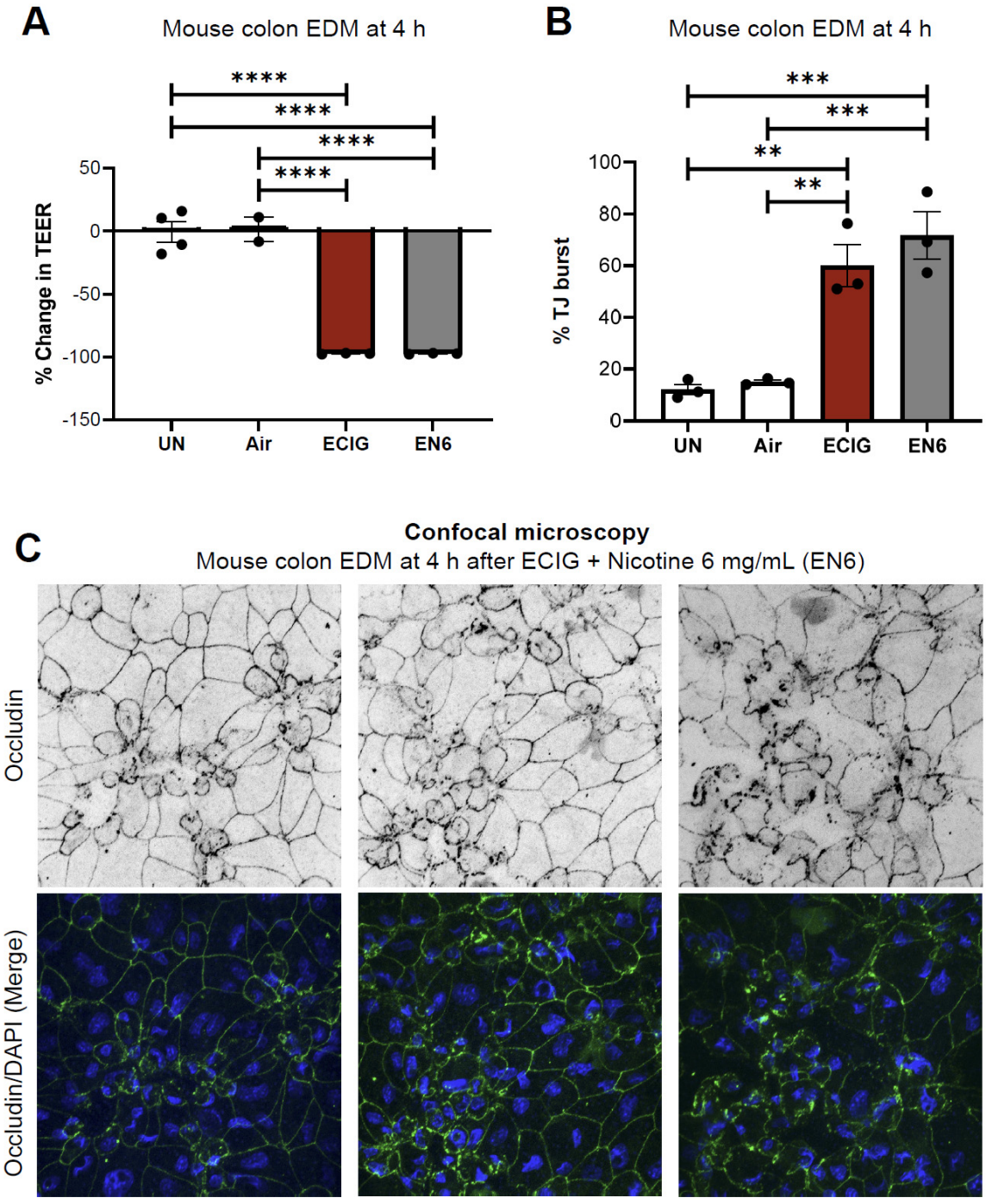


**Figure S6. Media infused with vapors from nicotine-containing e-cig disrupt the integrity of the murine gut barrier to an extent similar to nicotine-free e-cig (related to Fig 4). A**. Bar graphs display the percent change in TEER of murine EDMs after 4 h. EDMs were either grown in normal media (UN) or treated with air-infused media (Air) or e-cig vapor-infused media (ECIG) or e-cig with 6 mg/mL of nicotine vapor-infused media (EN6). Data is displayed as mean ± SEM (n = 3 independent experiments). **B-C.** EDMs were treated as indicated, fixed and stained for occludin (green) and DAPI (blue, nuclei) and analyzed by confocal microscopy. Bar graphs in **B** display the % increase in the tight junction (TJ) 'bursts' (indicative of disrupted TJs). Data is displayed as mean ± SEM (n = 3 fields/condition). Statistical significance was estimated using one-way ANOVA with Tukey's test; **$p < 0.01$, ,***$p < 0.001$ and ****$p < 0.0001$. Images in **C** display representative three different fields from EDMs after 4 h of treatment with e-cig containing 6 mg/mL of nicotine-infused media. Scale bar = 10 μm.

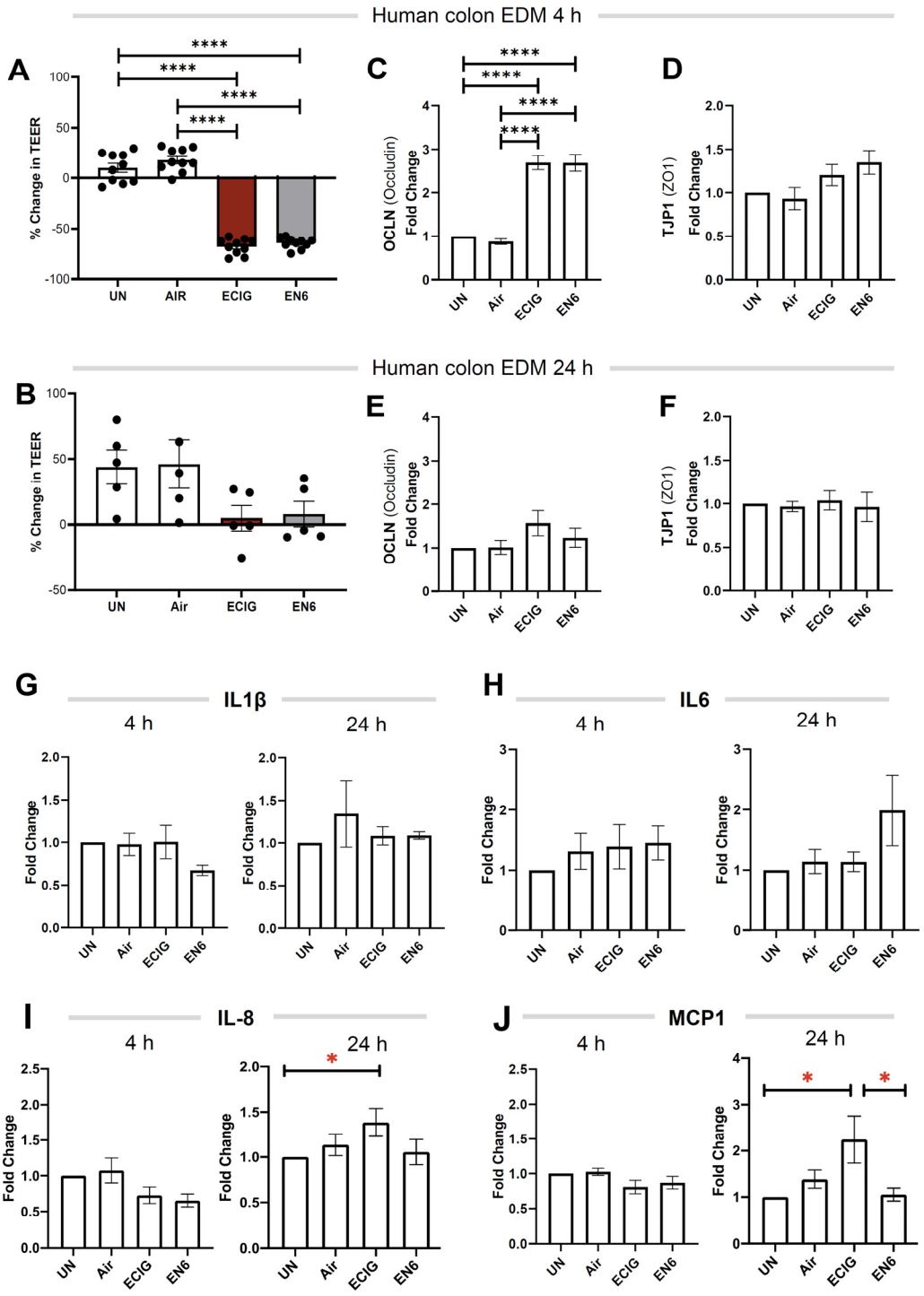


**Figure S7**. **Acute (4 h) and chronic (24 h) exposure to nicotine-free and nicotine-containing e-cigarettes decreases the TEER, alters the levels of markers of TJ and triggers inflammation to a similar extent (related to Fig 4).** (**A-B**) Bar graphs display the percent change in TEER of human colonic EDMs after 4 h (A) and 24 h (B) of the indicated treatments. EDMs were either grown in normal media (UN) or treated with air-infused media (Air) or e-cig vapor-infused media (ECIG) or e-cig with 6 mg/mL of nicotine vapor-infused media (EN6). Data is displayed as mean ± SEM (n = 5 independent experiments with 2 technical replicates for 4 h). (**C-F**) Bar graphs display the relative fold change in mRNA expression of TJ genes after 4 h (**C-D**) and 24 h (**E-F**) of the treatment. (**G-J**) Bar graphs display the relative fold change in mRNA expression of pro-inflammatory cytokines compared to the EDMs grown in normal media (UN) of genes from at least three independent experiments and displayed as mean ± SEM. One-way ANOVA with Tukey's test (black *) and Mann-Whitney (red *) test were performed. *$p < 0.05$, **$p < 0.01$ ***$p < 0.001$, ****$p < 0.0001$.

**SUPPLEMENTARY REFERENCES**


Bray, N.L., Pimentel, H., Melsted, P., and Pachter, L. (2016). Near-optimal probabilistic RNA-seq quantification. Nat Biotechnol *34*, 525-527.

Chassaing, B., and Darfeuille-Michaud, A. (2011). The commensal microbiota and enteropathogens in the pathogenesis of inflammatory bowel diseases. Gastroenterology *140*, 1720-1728.

Darfeuille-Michaud, A., Boudeau, J., Bulois, P., Neut, C., Glasser, A.L., Barnich, N., Bringer, M.A., Swidsinski, A., Beaugerie, L., and Colombel, J.F. (2004). High prevalence of adherent-invasive Escherichia coli associated with ileal mucosa in Crohn's disease. Gastroenterology *127*, 412-421.

Gao, X., Holleczek, B., Cuk, K., Zhang, Y., Anusruti, A., Xuan, Y., Xu, Y., Brenner, H., and Schottker, B. (2019). Investigation on potential associations of oxidatively generated DNA/RNA damage with lung, colorectal, breast, prostate and total cancer incidence. Sci Rep *9*, 7109.

Ghosh, P., Swanson, L., Sayed, I.M., Mittal, Y., Lim, B.B., Ibeawuchi, S.R., Foretz, M., Viollet, B., Sahoo, D., and Das, S. (2020). The stress polarity signaling (SPS) pathway serves as a marker and a target in the leaky gut barrier: implications in aging and cancer. Life Sci Alliance *3*.

Li, B., and Dewey, C.N. (2011). RSEM: accurate transcript quantification from RNA-Seq data with or without a reference genome. BMC Bioinformatics *12*, 323.

Miyoshi, H., and Stappenbeck, T.S. (2013). In vitro expansion and genetic modification of gastrointestinal stem cells in spheroid culture. Nat Protoc *8*, 2471-2482.

Pachter, L. (2011). Models for transcript quantification from RNA-Seq. In arXiv e-prints.

Rodrigues, D.G.B., de Moura Coelho, D., Sitta, A., Jacques, C.E.D., Hauschild, T., Manfredini, V., Bakkali, A., Struys, E.A., Jakobs, C., Wajner, M.*, et al.* (2017). Experimental evidence of oxidative stress in patients with l-2-hydroxyglutaric aciduria and that l-carnitine attenuates in vitro DNA damage caused by d-2-hydroxyglutaric and l-2-hydroxyglutaric acids. Toxicol In Vitro *42*, 47-53.

Sahoo, D., Dill, D.L., Tibshirani, R., and Plevritis, S.K. (2007). Extracting binary signals from microarray time-course data. Nucleic Acids Res *35*, 3705-3712.

Sato, T., Vries, R.G., Snippert, H.J., van de Wetering, M., Barker, N., Stange, D.E., van Es, J.H., Abo, A., Kujala, P., Peters, P.J.*, et al.* (2009). Single Lgr5 stem cells build crypt-villus structures in vitro without a mesenchymal niche. Nature *459*, 262-265.

Sayed, I.M., Chakraborty, A., Abd El Hafeez, A.A., A., S., Sahan, A.Z., WJM, H., Sahoo, D., Ghosh, P., Hazra, T.K., and Das, S. (2020a). The DNA Glycosylase NEIL2 Suppresses Fusobacterium-Infection-Induced Inflammation and DNA Damage in Colonic Epithelial Cells. Cells *9*.

Sayed, I.M., Sahan, A.Z., Venkova, T., Chakraborty, A., Mukhopadhyay, D., Bimczok, D., Beswick, E.J., Reyes, V.E., Pinchuk, I., Sahoo, D.*, et al.* (2020b). Helicobacter pylori infection downregulates the DNA glycosylase NEIL2, resulting in increased genome damage and inflammation in gastric epithelial cells. J Biol Chem *295*, 11082-11098.

Sayed, I.M., Suarez, K., Lim, E., Singh, S., Pereira, M., Ibeawuchi, S.R., Katkar, G., Dunkel, Y., Mittal, Y., Chattopadhyay, R.*, et al.* (2020c). Host engulfment pathway controls inflammation in inflammatory bowel disease. FEBS J *287*, 3967-3988.